AIP | Journal of Applied Physics

Effect of ZnO nanoparticles on the SmC*-SmA* phase transition temperature in electroclinic liquid crystals

A. Malik, A. Choudhary, P. Silotia, and A. M. Biradar

Citation: J. Appl. Phys. **110**, 064111 (2011); doi: 10.1063/1.3642087
View online: http://dx.doi.org/10.1063/1.3642087
View Table of Contents: http://jap.aip.org/resource/1/JAPIAU/v110/i6
Published by the American Institute of Physics.

Effect of ZnO nanoparticles on the SmC*-SmA* phase transition temperature in electroclinic liquid crystals

A. Malik,[1,2] A. Choudhary,[1] P. Silotia,[2] and A. M. Biradar[1,a)]
[1]*Liquid crystal and self assembled monolayer section, National Physical Laboratory, Dr. K. S. Krishnan Road, New Delhi 110012, India*
[2]*Department of Physics and Astrophysics, University of Delhi, Delhi 110007, India*

(Received 24 March 2011; accepted 16 August 2011; published online 23 September 2011)

ZnO nanoparticles (NPs), synthesized in an alcoholic medium at room temperature, were added to electroclinic liquid crystal (ELC) materials. The addition of ZnO NPs in ELCs, caused a remarkable shift in SmC*-SmA* phase transition which was investigated from the dielectric and electro-optical measurements. The anchoring of ELC molecules around ZnO NPs creates orientational distortions near the surface, which may give additional ordering to the ELC molecular arrangement. After analyzing collective dielectric relaxation processes of ZnO NP doped ELCs, three distinct loss peaks were observed. The different behavior of ZnO NP doped ELC from pure ELC has been explained by determining the dielectric strength, the distribution parameter and the corresponding relaxation frequency, and so on, and then these results have been compared with the data calculated by using the theoretical model. The effect of ZnO NPs addition on physical parameters, such as spontaneous polarization (P_s) and rotational viscosity (η) has also been observed. © *2011 American Institute of Physics*. [doi:10.1063/1.3642087]

I. INTRODUCTION

Nanoscience and nanotechnology are vital frontiers in scientific research. A broad area of research topics from fundamental physical, biological, and chemical phenomena to material science has been addressing by the scientific society at the nanoscale.[1–3] Nanoparticle doping technology provides a more convenient and flexible approach for the modification of liquid crystal (LC) materials and for designing new and improved devices based upon LCs. The minute addition of nanoparticles (NPs) to LC materials has improved many special characteristics in the form of frequency modulation response,[4] non-volatile memory effect,[5] fast electro-optic response,[6] low driving voltage,[7] and so on.

Of all the interesting materials emerging from the field of nanotechnology, metallic nanoparticles continue to attract immense research interest. Liquid crystal displays (LCDs) doped with metal NPs such as silver (Ag), gold (Au), palladium (Pd), platinum (Pt), or their alloys exhibited faster response times[8–12] than those of LCDs with conventional driving methods.

Zinc oxide nanoparticles (ZnO NPs) have attracted increasing attention owing to their wide application in nanogenerators,[13] gas sensors,[14] highly efficient solar cells, field-emission transistors,[15] ultraviolet photo detectors,[16] and in biomedical systems such as cancer detecting biosensors and ultra sensitive DNA sequence detectors.[17] Numerous research groups have explored how the addition of ZnO NPs in ferroelectric LCs (FLCs) mainly reduced the threshold voltage and improved the optical contrast of the LC display devices.[18,19] Huang *et al*. explored the effect of doping of ZnO NPs in surface stabilized ferroelectric liquid crystals (SSFLCs) by improving the alignment of FLC molecules and field induced reorientation processes.[20] Moreover, Li and Huang proposed a physical model depicting an interaction of ZnO NPs with surrounding FLC molecules.[21] But the effect of ZnO NPs on the phase transition temperature and dielectric relaxation processes of FLC materials has not been reported.

In the present study we have investigated the effect of ZnO NPs on the collective dielectric relaxation processes in electroclinic LCs (a special type of FLCs).[22] The experiments have been carried out on planarly aligned sample cells. Three distinct loss peaks in the SmC* phase of ZnO NP doped ELC have been observed near the transition temperature (T_c) between ferroelectric SmC* and paraelectric SmA* phases, which were not present in the pure ELC material. It has also been observed that the doping of ZnO NPs in ELC (BDH 764E) enhanced the transition temperature T_c because of the significant strength of interaction between ZnO NPs and ELC molecules. The comparable enhancement in T_c with ZnO NPs has also been checked in another ELC material, Felix-20. The results have also been compared with the data calculated by using the theoretical model (Cole-Cole model). The effect of doping on the physical characteristics of materials such as spontaneous polarization (P_s) and rotational viscosity (η) has also been discussed.

II. EXPERIMENT

The ZnO NPs used in the present study were synthesized in an alcoholic medium at room temperature by using zinc acetate and lithium hydroxide. The characteristic size of synthesized ZnO NPs estimated by x-ray diffraction pattern was found to be around 7 nm. The x-ray diffraction pattern of the present ZnO NPs has been reported earlier.[19]

For the thermal and dielectric studies of the ELC material, the LC sample cells were prepared by using transparent

a)Author to whom correspondence should be addressed. Electronic mail: abiradar@mail.nplindia.ernet.in.

and highly conducting indium tin oxide (ITO, with sheet resistance 20 Ω/□) coated glass substrates that acted as electrodes. The electrodes were treated with adhesion promoter (phenyl trichlorosilane in toluene) followed by polymer (nylon 6/6) coating and were unidirectionally rubbed to get planar alignment of ELC molecules. The glass substrates were assembled with the electrodes facing each other, in the form of cells, maintaining a uniform thickness of around 3 μm.

The commercially available ELC material used in our present study is BDH 764E and the phase sequence is as follows:

$$\text{Cryst.} \overset{-7\,^{\circ}\text{C}}{\longleftrightarrow} \text{SmC}^{*} \overset{28\,^{\circ}\text{C}}{\longleftrightarrow} \text{SmA}^{*} \overset{73\,^{\circ}\text{C}}{\longleftrightarrow} \text{N} \overset{89-92\,^{\circ}\text{C}}{\longleftrightarrow} \text{Iso.}$$

A small amount (1 wt. %) of ZnO NPs was doped in to the ELC material and then the ZnO doped ELC material was introduced into the cell by means of capillary action at elevated temperature (~95 °C) to ensure that filling takes place in the isotropic phase.

The molecular and collective dielectric studies were carried out by dielectric spectroscopy in a shielded liquid crystal cell using a Wayne Kerr 6540 A impedance analyzer in the frequency range of 20 Hz to 1 MHz. The dielectric setup was fully computer controlled and automated. The sample temperature was controlled within the accuracy of ± 0.01°C using a JULABO F-25 HE temperature controller. Optical tilt angle measurements were taken with the sample cell mounted on a rotatable stage of the polarizing optical microscope (Axioskop-40) interfaced with a Canon digital camera. Automatic liquid crystal tester (ALCT-P), which works on the principle of current measurement with time on the application of a triangular pulse,[23] was used for measuring spontaneous polarization (P_s) and rotational viscosity (η). The sample holder was kept thermally and electrically isolated from the outer sources.

III. RESULTS AND DISCUSSIONS

Addition of ZnO NPs to the pure ELC material results in the redistribution of intermolecular interaction energies, which can affect almost all of the physical parameters of the pure material. Dielectric relaxation spectroscopy is an important tool to study the molecular relaxation and dielectric properties of materials. Temperature dependence of dielectric relaxation can be described by the Debye theory but if collective dielectric processes exhibit a continuous distribution of relaxation time for liquid crystals then it can be described by the Cole-Cole equation, as given by

$$\varepsilon*(\omega) = \varepsilon_{\infty} + \sum_{i=1,2\ldots} \frac{(\varepsilon_o^i - \varepsilon_{\infty}^i)}{1 + (i\omega\tau_i)^{1-\alpha_i}} \qquad (1)$$

where ε_0, ε_∞, and τ stand for the static dielectric permittivity, frequency independent permittivity at high frequency, and relaxation time, respectively. i represents the number of relaxation processes and α stands for the distribution parameter. α is a measure of the width of the relaxation distribution and if the value of α is very small or equal to zero then the above Cole-Cole equation will obey the Debye process. The real and imaginary parts of permittivity can be separated out easily from the complex function by the relation

$$\varepsilon'(\omega) - j\varepsilon''(\omega) - j\varepsilon(\omega) \qquad (2)$$

where ε' denotes the real part of the complex dielectric permittivity, ε'' is the imaginary part of the permittivity, and ω is the angular frequency of applied electric field.

For the comparative studies, we prepared two sample cells, one with ZnO NP doped ELC material and another of pure ELC material. Figure 1(a) shows the real part of the dielectric constant (ε') as a function of frequency for a large temperature range of ELC material doped with ZnO NPs, while the ε' of pure ELC material is shown in the inset of Fig. 1(a) where the solid lines represents the best theoretically fit data using the Cole-Cole model. As seen from the inset, the ε' of pure ELC material continuously decreases in the SmC^* phase near the transition temperature of SmC^* to SmA^* (29 °C). The value of ε' in ELC is very high at lower frequencies (tens of Hz) and almost constant at higher frequencies (tens of KHz) in SmC^* and SmA^* phases.

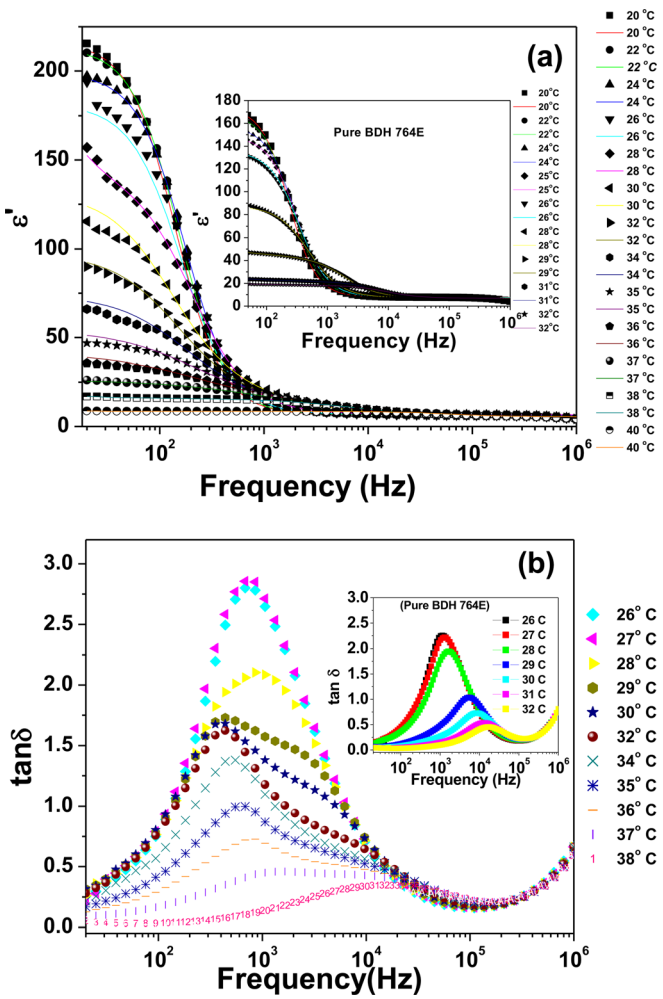

FIG. 1. (Color online) Frequency dependences of dielectric permittivity ε' (a) and tan δ (loss factor) (b) for electroclinic material (ELC) BDH764E at different temperatures. Main plots: ELC is doped with 1 wt. % of ZnO nanoparticles. Insets: un-doped material. Solid lines in **(a)** represent the calculated data. No bias field.

The ELC material doped with ZnO NPs shows a drastic change in the dielectric relaxation processes, as shown in Fig. 1(a). The high dielectric permittivity (ε') is due to the Goldstone mode in SmC* phase appearing up to 36 °C. The phase transition temperature T_c between SmC* and SmA* phases can be varied by variation of the concentration c of ZnO NPs in ELC material. In our study, we have found the maximum shift in T_c at concentration c of ZnO NPs around 1 wt. %. For further increase of c the shift of the transition temperature T_c decreases. At $c > 2$ wt. %, there is no significant shift of T_c in comparison with the un-doped case.

Figure 1(b) shows the behavior with temperature of tan δ versus frequency of a ZnO NP doped ELC sample while the inset of this figure shows the behavior of tan δ versus frequency of pure ELC material at the same parameters. From these graphs also, one can confirm the change in phase transition temperature T_c. From the inset of Fig. 1(b), an abrupt increase in the value of the relaxation frequency near 29 °C can be seen for pure ELC, while for ZnO NP doped ELC the increase in relaxation frequency is at about 36 °C [Fig. 1(b)]. In the SmC* phase there are two or more relaxation peaks present in ZnO NP doped ELCs, which were totally absent in pure ELC material as well as at c exceeding 2 wt. %. The edge of the high frequency dielectric loss above 100 KHz in Fig. 1(b) occurs due to the finite resistance of the ITO coating on the glass substrate of the sample cell. This ITO effect on dielectric measurements also has been reported elsewhere.[24]

Figure 2(a) shows the Cole-Cole diagrams at two different temperatures, one in the SmC* phase (2° below T_c) and another in the SmA* phase (2° above T_c) for ZnO NP doped ELC material, while Fig. 2(b) shows the Cole-Cole plots for pure ELC material 2° below T_c in SmC* and 3° above T_c in SmA* phases, respectively. In Fig. 2(a), at lower temperature (34 °C) by fitting the expression of Eq. (1), one can observe that the Cole-Cole diagram is a superposition of two semicircles, i.e., at this temperature two modes are contributing to the dielectric response while at higher temperature (38 °C), only one relaxation behavior is present, which is attributed to the soft mode in he case of ZnO doped ELC material. Figure 2(b) shows the Cole-Cole diagrams at two different temperatures (26 °C and 31 °C) for pure ELC material, in which only a single relaxation behavior is present.

The behavior of relaxation frequency ($\nu_{R,\varepsilon''}$) in SmC* and SmA* phases has been shown in Fig. 3(a), calculated by the formula $\nu_{R,\varepsilon''} = \nu_{R,\tan\delta}\sqrt{\varepsilon_\infty/\varepsilon_o}$.[25] Figure 3(a) shows the relaxation frequency versus temperature for ZnO NP doped ELC and the inset shows the same for pure ELC material, without any bias application. The solid line represents the best theoretically calculated data by using the Cole-Cole model through the experimental points. As seen from the inset of Fig. 3(a), the relaxation frequency is found to be independent of temperature in the deep SmC* phase and at the transition from SmC* to SmA* phase there is a continuous increment in the value of the relaxation frequency for pure ELC material. In the case of ZnO NP doped ELC material as we discussed earlier in Fig. 1(b), there are two relaxation peaks. In Fig. 3(a) the behavior of both relaxation peaks has been shown with respect to temperature. The solid lines of

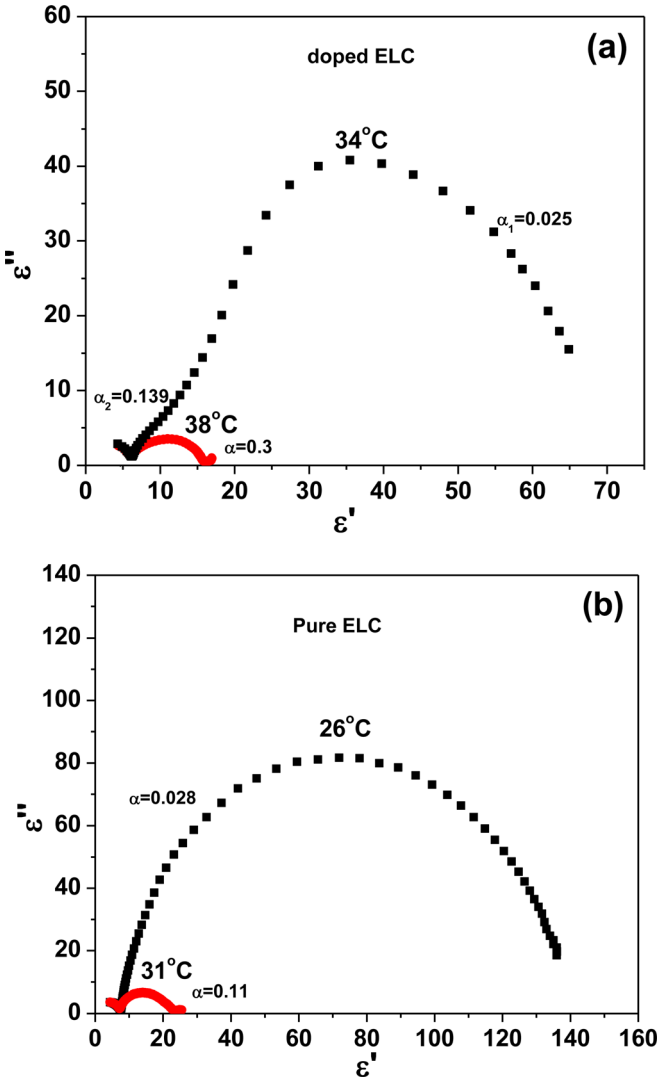

FIG. 2. (Color online) (a) The Cole-Cole plots of the ZnO NP doped ELC (1 wt. %) for SmC* (34 °C) and SmA* (38 °C) phases, (b) The same as in (a) but for pure ELC in SmC* (26 °C) and SmA* (31 °C). No bias field.

theoretically calculated and experimental data are almost matching with each other. The frequency separation of both relaxation peaks increases with an increase in temperature and the peak along with the low frequency side almost vanishes above the transition temperature T_c in NP doped ELC material. Only the regular soft mode process remains above T_c, showing the usual behavior of ELC materials. Such a type of low frequency relaxation peak has also been observed in water added and graphene oxide added ELC samples.[26,27]

The experimentally obtained values of dielectric strength $\Delta\varepsilon$, distribution parameter α, and the corresponding relaxation frequency $\nu_{R,\varepsilon''}$ in a wide temperature range have been given in Table I and Table II for both pure and doped ELC materials and compared to the data calculated by using the Cole-Cole theoretical model. One can observe from Tables I and II that there is an increase of the distribution parameter α with respect to temperature. The small values of α for both pure and ZnO NP doped ELC suggest that the dielectric process is very close to Debye type relaxation. The

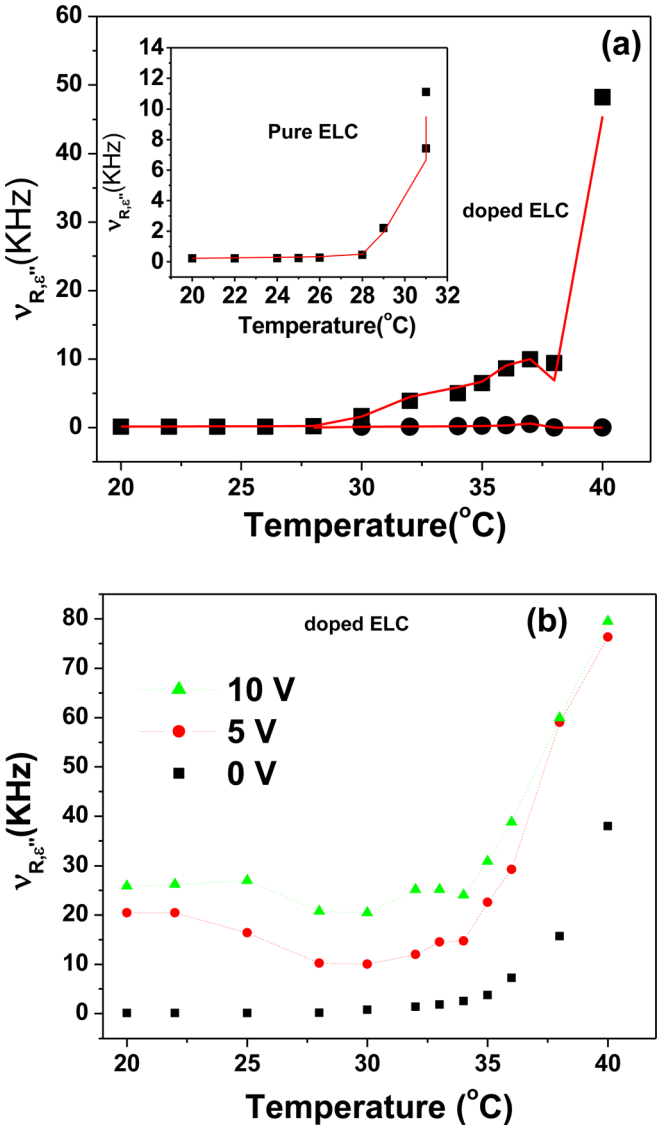

FIG. 3. (Color online) (a) Behavior of relaxation frequencies with respect to temperatures for ZnO doped ELC (main plot) and for pure ELC sample (inset). No bias field. Filled squares show the experimental points for first dielectric process and filled circles for the second dielectric process. Solid lines represents the theoretically calculated data for the first and second dielectric processes by using the Cole-Cole equation. (b) The experimental behavior of relaxation frequency with different bias (0 V, 5 V, and 10 V) for ZnO doped ELC.

increase of α with temperature indicates that both samples become less dispersive at higher temperatures and must show more than one relaxation process at some higher temperatures in the SmC^* phase.

In Fig. 3(b), the relaxation frequency has been plotted with respect to temperature for ZnO NP doped ELC material at different bias voltages (0 V, 5 V, and 10 V). The behavior of $\nu_{R,\varepsilon''}$ at 0 V bias for pure and ZnO NP doped ELC is the same, for instance far below the transition temperature T_c,$\nu_{R,\varepsilon''}$ is independent of temperature and approaching the T_c transition there is a continuous increase of $\nu_{R,\varepsilon''}$. At bias voltages (5 V and 10 V) in the deep SmC^* phase the relaxation frequency $\nu_{R,\varepsilon''}$ is almost independent of temperature but decreases in the interval 25–30 °C and increases at approaching the transition temperature T_c. After transition temperature there is an abrupt increase in the value of $\nu_{R,\varepsilon''}$. The behavior of $\nu_{R,\varepsilon''}$ with bias in ZnO NP doped ELC material is similar to pure ELC and it does not obey the Curie-Weiss law in the SmC^* phase due to high electroclinic coefficient of such ELC materials. Thakur *et al*. have reported earlier that pure ELC materials do not obey the Curie-Weiss law near the transition temperature.[28] In the SmA^* phase the relaxation frequency is temperature dependent, as in other FLC materials.

The bias-dependent relaxation processes have been studied for the SmC^* phase of ZnO NP doped and pure material (inset), as shown in Fig. 4(a). Figure 4(a) shows the behavior of dielectric loss (tan δ) curve at different applied biases for both doped and pure material. At lower bias voltages (in the range of 0.1 V to 1 V) in the SmC^* phase, we see two or more than two low frequency relaxation peaks in the case of ZnO NP doped ELC samples, which can also be confirmed by Fig. 4(b). Figure 4(b) shows the Cole-Cole plot at 0.3 V in the SmC^* phase (29°C) for ZnO NP doped ELC material. The Cole-Cole semicircles also show the presence of more than two relaxation behaviors. The inset of Fig. 4(b) shows the theoretical fitting for the same data and also exhibits the three relaxation processes (three different values of distribution parameter α) while the pure sample exhibits only one relaxation process due to a characteristic Goldstone mode, as shown in the inset of Fig. 4(a). The appearance of two or more than two relaxation peaks with the application of bias in the SmC^* phase suggests that there is a strong interaction

TABLE I. Variation of dielectric strength, distribution parameter, and relaxation frequency with temperature for pure ELC material and comparison with theoretically calculated data.

Temperature (°C)	$\Delta\varepsilon$	α (Experimental)	α (Theoretical)	$\nu_{R,\varepsilon''}$ (KHz) (Experimental)	$\nu_{R,\varepsilon''}$ (KHz) (Theoretical)
20	166.25	0.011	0.010	0.222	0.232
22	161.56	0.017	0.030	0.225	0.256
24	150.33	0.022	0.032	0.232	0.294
25	138.70	0.022	0.035	0.241	0.312
26	128.47	0.028	0.045	0.268	0.333
27	109.45	0.028	0.050	0.322	0.335
28	83.65	0.031	0.074	0.453	0.498
29	40.75	0.033	0.08	2.205	1.923
30	28.86	0.100	0.090	3.674	3.122
31	18.16	0.110	0.096	7.420	6.670
32	12.66	0.144	0.100	11.110	9.523

TABLE II. Variation of dielectric strength, distribution parameter, and relaxation frequency with temperature for ZnO NP doped ELC material and comparison with theoretically calculated data.

Temperature (°C)	$\Delta\varepsilon$	α (Experimental)		α (Theoretical)		$\nu_{R,\varepsilon''}$ (KHz) (Experimental)		$\nu_{R,\varepsilon''}$ (KHz) (Theoretical)	
20	209.01	0.011		0.010		0.120		0.140	
22	203.85	0.017		0.017		0.120		0.150	
24	190.70	0.028		0.020		0.124		0.172	
25	190.03	0.028		0.026		0.124		0.183	
26	187.57	0.033		0.032		0.125		0.200	
27	176.59	0.033		0.034		0.128		0.200	
28	150.61	0.056		0.065		0.183		0.208	
30	109.11	0.011	0.056	0.020	0.080	0.103	1.680	0.127	1.600
32	83.70	0.022	0.133	0.030	0.140	0.122	3.890	0.161	4.454
34	59.83	0.025	0.139	0.035	0.140	0.170	5.010	0.192	5.879
35	40.66	0.028	0.139	0.058	0.190	0.250	6.500	0.220	6.676
36	29.30	0.031	0.144	0.068	0.200	0.354	8.630	0.300	9.069
37	19.88	0.033	0.278	0.080	0.330	0.520	9.990	0.580	9.990
38	10.74	0.300		0.260		9.401		6.900	
40	3.62	0.310		0.220		48.230		45.450	

between the ZnO NPs and molecules of ELCs and the low frequency process is associated with the Goldstone mode of ELC material.

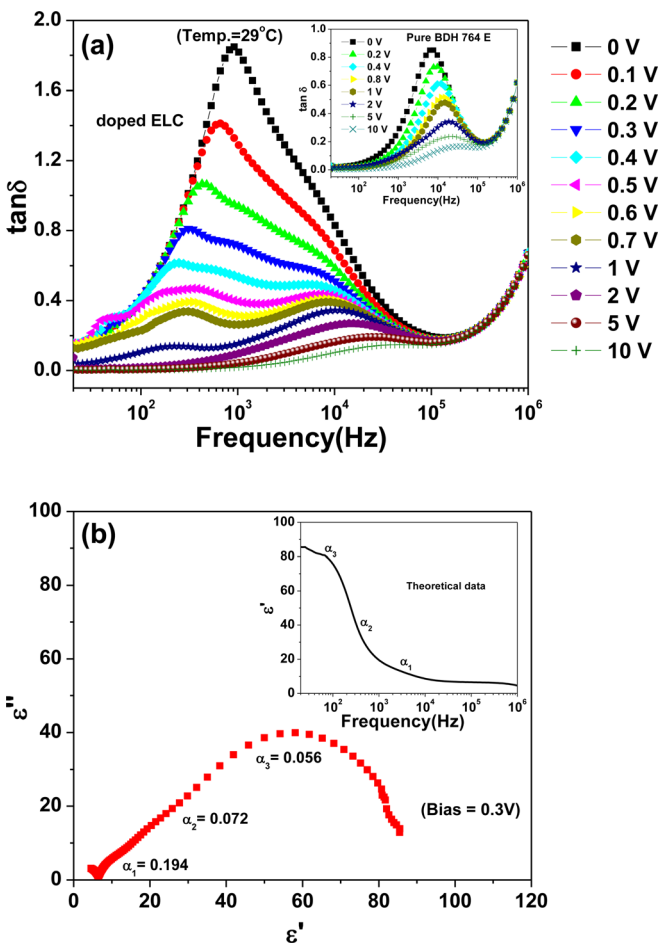

FIG. 4. (Color online) (a) Behavior of dielectric loss factor (tan δ) for ZnO doped ELC and in the inset, for pure ELC material, with frequency at different values of applied voltages at 29 °C, while (b) shows the Cole-Cole plot for the ZnO doped ELC at 0.3 V bias and in the inset the solid line shows the theoretical calculated data for the same experimental data.

Figure 5(a) shows the plot of the measured temperature dependence of the tilt angle for both pure and ZnO doped ELC materials. There is no remarkable difference in the temperature dependent tilt angle measurement of pure and ZnO doped ELC. This is because the ZnO NPs have suppressed the randomized scattering of ELC molecules around a diffuse cone but the tilt of the individual molecules remains the same. The phase of ELC has been extended by ZnO only in the limit of the electroclinic effect in the SmA^* phase, therefore the larger the electroclinic effect the greater the phase extension (increase of T_c from SmC^* to SmA^* phases). The phase extension has been observed only in ELCs and not in conventional FLCs.

Figure 5(b) shows the variation in the ratio of polarization and optical tilt angle (P_s/θ) with respect to temperature for both pure and ZnO doped ELC materials. There is a rapid fall in the value of P_s/θ for pure material as compared to ZnO NP doped material. ZnO NP doped ELC shows a gradual fall in the P_s/θ value, which suggests a rise in the order of ELC molecules. From the inset of Fig. 5(b) it can be observed that there is an improvement in the polarization (P_s) by doping ZnO NPs in ELC as compared to the pure material with respect to temperature. The improved P_s is due to the arrangement of dipole moments of ZnO NPs in the direction of the applied field, which will contribute to the dipole moment of pure ELC material. Hence, the ratio of polarization and tilt angle (P_s/θ) will be more in the case of ZnO NP doped ELC material. One can also validate the shift in SmC^* to SmA^* phase transition temperature T_c in the ZnO NP doped ELC material from Fig. 5(b).

Figure 6 shows the variation in rotational viscosity (η) with respect to temperature without any bias application. There is an increase in rotational viscosity (η) in ZnO NP doped ELC as compared with pure ELC. The increment in η decreases with respect to temperature, which means as we increase the temperature the gap between the value of η in the case of pure and ZnO NP doped ELCs decreases. This increment of η is a result of the strong interaction between ZnO NPs with ELC molecules and the possible formation of clusters.

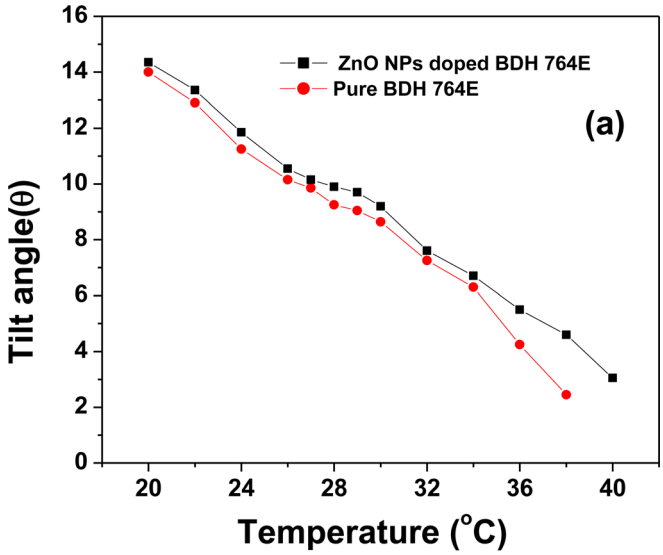

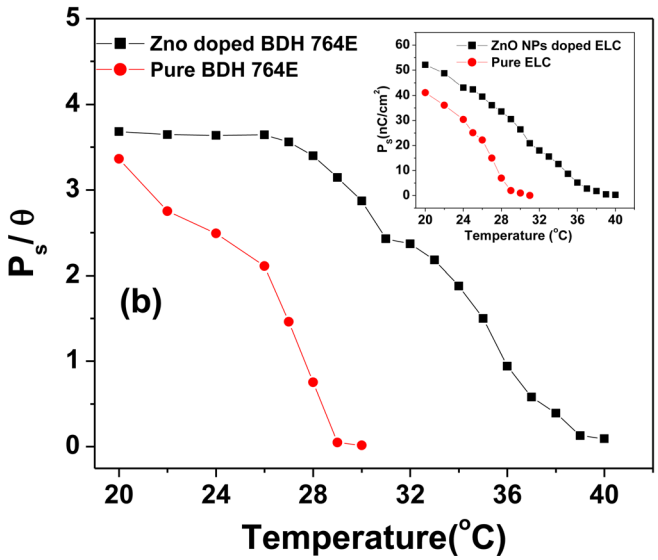

FIG. 5. (Color online) (a) Behavior of tilt angle theta with respect to temperature for both ZnO doped and pure ELC samples while (b) shows the behavior of the ratio of P_S/θ with respect to temperature and in the inset, the behavior of spontaneous polarization (P_S) with temperature for both ZnO doped and pure ELC samples.

The value of the dipole moment of ELC molecules ($>$1.5 D) is very small as compared with ZnO NPs ($>$100 D) and the huge dipole moment of the ZnO NPs generates a powerful field inducing dipolar interaction that competes with spontaneous molecular interaction and this dipolar interaction enhances the anchoring of ELC molecules around ZnO NPs. Such strong anchoring of ELC molecules around ZnO NPs brings about long range orientational distortions, which may give rise to the well ordered molecular structure of ELC materials and enhance the ferro- to paraelectric phase transition temperature. In our earlier study, when we doped the ELC material by a non dipolar organic material (heptane), there was no additional dielectric peak while by adding a dipolar material (graphene oxide nanomaterial) we observed one additional peak along with the Goldstone mode.[27] The interaction between ELC molecules and NPs

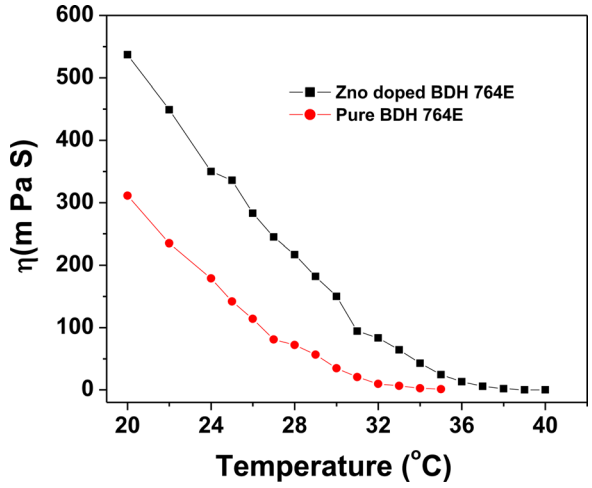

FIG. 6. (Color online) Behavior of rotational viscosity (η) with respect to temperature for both ZnO doped and pure ELC sample cells.

with large dipole moments also affects the dielectric relaxation processes in ELCs.

IV. CONCLUSIONS

We have demonstrated that the transition temperature of ferro- to paraelectric phase of ELC materials can be increased by the doping of ZnO NPs. As a result of the large dipole moment of ZnO NPs, a strong molecular interaction takes place between ZnO NPs and ELC molecules, which can give rise to the order of ELC molecules. Our experimental outcomes illustrate the existence of one or more than one additional low frequency relaxation peak along with the Goldstone mode in the SmC* phase and these relaxation peaks vanish after the transition temperature. The doping of 1 wt. % of ZnO NPs makes a significant increase in the values of P_S and η in ELC material. This work is also helpful for various dynamic studies of ELCs and opens up innovative ways to implement ELCs for potential applications at higher temperature.

ACKNOWLEDGMENTS

The authors sincerely thank the Director of the National Physical Laboratory, Professor R. C. Budhani, for continuous encouragement and interest in this work. The authors are also thankful to Dr. Jai Prakash (IIT Delhi) for his fruitful discussions. The authors (A.M. and A.C.) are thankful to CSIR, New Delhi for financial assistance.

[1]W. H. De Jong and P. J. A. Borm, Int. J. Nanomedicine **3**, 133 (2008).
[2]G. Reiss and A. Hutten, Nature Mater. **4**, 725 (2005).
[3]J. F. Scott, *Ferroelectric Memories* (Berlin, Springer, 2000), pp. 191–206.
[4]Y. Shiraishi, N. Toshima, K. Maeda, H. Yoshikawa, J. Xu, and S. Kobayashi, Appl. Phys. Lett. **81**, 2845 (2002).
[5]J. Prakash, A. Choudhary, A. Kumar, D. S. Mehta, and A. M. Biradar, Appl. Phys. Lett. **93**, 112904 (2008).
[6]J. Prakash, A. Choudhary, D. S. Mehta, and A. M. Biradar, Phys. Rev. E **80**, 012701 (2009).
[7]W. Lee, C. Y. Wang, and Y. C. Shih, Appl. Phys. Lett. **85**, 513 (2004).
[8]N. Mizoshita, K. Hanabusa, and T. Kato, Adv. Funct. Mater. **13**, 313 (2003).
[9]J. Thisayukta, H. Shiraki, Y. Sakai, T. Masumi, S. Kundu, Y. Shiraishi, N. Toshima, and S. Kobayashi, Jpn. J. Appl. Phys. **43**, 5430 (2004).

[10]H. Shiraki, S. Kundu, Y. Sakai, T. Masumi, Y. Shiraishi, N. Toshima, and S. Kobayashi, Jpn. J. Appl. Phys. **43**, 5425 (2004).
[11]H. Yoshikawa, K. Maeda, Y. Shiraishi, J. Xu, H. Shiraki, N. Toshima, and S. Kobayashi, Jpn. J. Appl. Phys. **41**, L1315 (2002).
[12]Y. Sakai, N. Nishida, H. Shiraki, Y. Shiraishi, T. Miyama N. Toshima, and S. Kobayashi, Mol. Cryst. Liq. Cryst. **441**, 143 (2005).
[13]X. Wang, J. Song, and Z. L. Wang J. Mater. Chem., **17**, 711 (2007).
[14]N. Hongsith, C. Viriyaworasakul, P. Mangkorntong, N. Mangkorntong, and S. Choopun, Ceram. Int. **34**, 823 (2008).
[15]M. S. Arnold, P. Avouris, Z. W. Pan, and Z. L. Wang, J. Phys. Chem. B **107**, 659 (2003).
[16]J. H. Jun, H. Seong, K. Cho, B. M. Moon, and S. Kim, Ceram. Int. **35**, 2797 (2009).
[17]N. Kumar, A. Dorfman, and J. I. Hahm, Nanotechnology **17**, 2875 (2006)
[18]H. Jiang and N. Toshima, Chem. Lett. **38**, 566 (2009).
[19]T. Joshi, A. Kumar, J. Prakash, and A. M. Biradar, Appl. Phys. Lett. **96**, 253109 (2010).
[20]J. Y. Huang, L. S. Li, and M. C. Chen, J. Phys. Chem. C **112**, 5410 (2008).
[21]L. S. Li and J. Y. Huang, J. Phys. D: Appl. Phys. **42**, 125413 (2009).
[22]S. Garroff and R. B. Meyer, Phys. Rev. Lett. **38**, 848 (1977).
[23]K. Miyasato, S. Abe, H. Takezoe, A. Fukuda, and E. Kuze, Jpn. J. Appl. Phys. **22**, L661 (1983).
[24]F. Gouda, K. Skarp, and S. T. Lagerwall, Ferroelectrics **113**, 165 (1991).
[25]A. Chelkowski, *Dielectric Physics* (New York, Elsevier Scientific, 1980).
[26]G. Singh, A. Choudhary, G. Vijaya Prakash, and A. M. Biradar, Phys. Rev. E **81**, 051707 (2010).
[27]A. Malik, A. Choudhary, P. Silotia, A. M. Biradar, V. K. Singh, and N. Kumar, J. Appl. Phys. **108**, 124110 (2010).
[28]A. K. Thakur, G. K. Chadha, S. Kaur, S. S. Bawa, and A. M. Biradar, J. Appl. Phys. **97**, 113514 (2005).